Sodium hydride NaH(X1Σ+) in collision with helium He(1S) at low temperature: Potential energy surface and rotational rate coefficients

Cheikh Bop, N. P. Faye, K. Hammami

Sodium hydride NaH($X^1\Sigma^+$) in collision with helium He(^1S) at lowtemperature: Potential energy surface and rotational rate coefficients

Cheikh T. Bop,[1, a)] N. A. B. Faye,[1, b)] and K. Hammami[2, c)]
[1)] *Laboratory of Atoms Lasers, Department of Physics, Faculty of Sciences and Techniques, University Cheikh Anta Diop of Dakar*
[2)] *Laboratory of Atomic Molecular Spectroscopy and Applications, Department of Physics, Faculty of Sciences, University Tunis El Manar, Campus Universities, 1060, Tunis, Tunisia*

(Dated: 30 August 2018)

The ro-vibrational transitions of sodium hydride (NaH) are crucially needed for the control of photo-association processes resulting from its formation as well as for accurately modeling the NaH abundance in space. In this work, we constructed new PESs (in the NaH equilibrium geometry, averaged geometry and by taking into account the NaH stretching) of the NaH($X^1\Sigma^+$)−He(^1S) van der Waals collisional system. The interaction potentials were computed with the explicitly correlated coupled cluster ab initio approach with simple, double and perturbative triple excitation (CCSD(T)–F12) in conjunction with the correlation consistent–polarized valence triple zeta Gaussian basis set (cc-pVTZ). Each of the three PESs presents two local minima of ∼12.9 cm^{-1} and ∼2.7 cm^{-1}. From these interaction potentials, we calculated rotational cross sections of NaH induced by collision with He for energies up to 1500 cm^{-1} using the exact quantum mechanical close coupling approach. These cross sections were averaged at low temperature (T ≤ 200 K) to obtain the collisional rates involving the 11 first rotational levels of NaH. The data obtained using the different computed PESs are very similar. The propensity rules favorite odd Δj transitions. The collisional rates presented in this paper may be crucial for the astrophysical community in case NaH would be observed in space. The three dimensional PES can be used later to compute ro-vibrational quenching rate coefficients to interpret the NaH collisional interaction with laser-cooled atoms.

I. INTRODUCTION

The chemistry of sodium (Na) is a particular interest for the astrophysical community. It is assumed to play a crucial role for the regulation of the fractional ionization in dense molecular clouds[1] which has a high impact in the ion-molecule chemistry[2]. An important fraction of interstellar Na is expected to be stored in sodium hydride (NaH). This latter is mainly formed in gas-phase sequence, more explicitly through radiative association (equation 1) followed by dissociative recombination (equation 2).

$$Na^+ + H_2 \longrightarrow NaH_2^+ + h\nu \tag{1}$$

$$NaH_2^+ + e \longrightarrow NaH + H \tag{2}$$

In diffuse clouds, atomic sodium exists mainly in the ionized form (Na^+) making the above pathway favourable. The alternative NaH production (i.e. formation on grain surfaces) is expected to produce less sodium hydride compared to the gas-phase results. However, it yields a detectable amount of NaH[3]. The so produced NaH is likely to immediately leave the grain[4] as it is, like lithium hydride (LiH) and potassium hydride (KH), chemically saturated. Basing to alkali metals cosmic abundances, NaH is believed to be the most abundant alkali hydride in space. In one hand, sodium hydride has a large permanent electric dipole moment (6.40 D)[5] making it an ideal candidate in radioastronomy. In another hand, the rotational emissions of NaH are expected to produce intense radiative transitions in the microwave and infrared regions. Both items along with the improved sensitivity of newer instruments (such as ALMA and APEX) let us expect that the coming tentative of detection of NaH will be fruitful.

Due to its large permanent electric dipole moment, sodium hydride is an ideal candidate for the chemistry of cold and ultracold molecules. Photoassociation (PA) is an accurate technique to produce cold and ultracold molecules. In a femtosecond laser field, sodium (Na) and hydrogen (H) combine to form NaH. In fact, the laser control of molecular and atomic dynamics became an active and interesting research topic.[6] Numerous experimental and theoretical schemes have been reported in the literature in order to control such a PA process.[7–9] In photochemistry, the collision of sodium and molecular hydrogen (H_2) is one of the most relevant atom-molecule systems. Therefore, NaH plays an important role in various fields and has been intensively studied.

Since the early 1970s, sodium hydride has been the subject of various investigations. Numerous experimental studies on the NaH ground state have been reported[10–12]. Ab initio calculations have been performed to study the Na + H and Na^+ + H^- collisions[13,14]. Reactive collisions involving NaH (such as equation 3) have been extensively investigated, theoreti-

[a)] Electronic mail: cheikhtidiane.bop@ucad.edu.sn
[b)] Electronic mail: arameboye.faye@ucad.edu.sn
[c)] Electronic mail: hammami283@gmail.com.

cally as well as experimentally[15–17], while ro-vibrational collisions have received little attention.

$$Na(3p) + H_2(v, j) \longrightarrow Na(3s) + H2(v', j') \longrightarrow NaH(v'', j'') + H \quad (3)$$

In the theoretical framework, NaH is an excellent prototype to probe the vibrational effects of light hydrides in rotational energy transfer. Lanza et al. showed that the global minimum of the HCl-He interaction potential varies weakly with the HCl bond stretching.[18] Kalugina et al. suggested to use vibrationally-averaged PESs instead of rigid-rotor PESs for a better description of experimental data.[19] Bouhafs et al. mentioned that state-averaged geometries are reliable approximations in order to take into account the vibrational effects with rigid-rotor PESs.[20] All these findings support that rigid-rotor interaction potentials constructed using experimental equilibrium geometries are not suitable to generate reliable collisional data. Therefore, to give a better insight of rigid-rotor potentials accuracy, we computed new PESs of the NaH-He system using state of the art approach. We have constructed a vibrationally averaged potential (vib–av–PES) and two rigid-rotor PESs. These latter were computed using the experimental equilibrium distance (r_e–PES) and the averaged distance (r_0–PES) of NaH respectively.

This paper is organized as follows: Section II presents the potential energy surfaces, Sections III stands for the details of the scattering calculations and in Section IV are given the concluding remarks.

II. INTERACTION POTENTIALS

An ab initio three-dimensional PES of the NaH-He van der Waals system was calculated using the CCSD(T)/CBS level of theory implemented in GAUSSIAN 98.[27] The Complete Basis Set (CBS) was generated from triple and quadruple zeta basis sets (without bond functions) using the equation of Martin.[29] To enable reliable comparisons in order to probe vibrational effects, we have computed new potentials of the system mentioned above.

In this work, the vib-av-PES is derived from an interaction potential described with three coordinates, namely, the NaH internuclear distance r, the distance between the NaH centre of mass and the He atom R and the scattering angle θ. We present in Fig. 1 the body-fixed Jacobi coordinate system. The NaH internuclear distance was assigned to 5 values (r = 2.85, 3.01, 3.57, 4.12 and 4.26 a_0). Thus, the NaH stretching between the classical turning points corresponding to the vibrational level $v = 2$ can be correctly taken into account. The distance R was varied from 4 to 30 a_0 using an irregular step size as follows: for $4.00 \leq R \leqslant 15.00$ a_0 the step was set to 0.25 a_0, to 0.50 a_0 for $15.00 \leq R \leqslant 20.00$ a_0 and to 1.00 a_0 for $20.00 \leq R \leqslant 30.00$ a_0. In addition, the potential was calculated at R = 100 a_0 to check on the asymptotic behaviour.

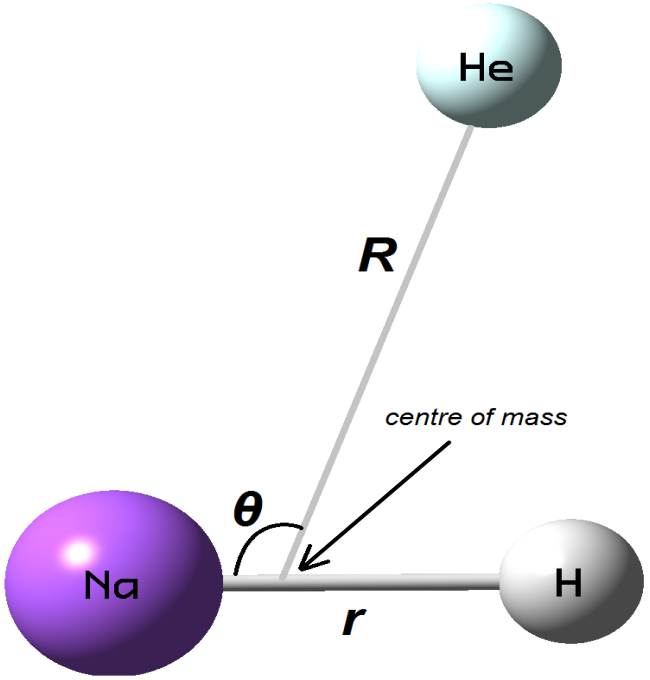

FIG. 1. Definition of the body-fixed Jacobi coordinate system for the NaH-He collisional complex.

The scattering angle θ was varied from 0 to 180° with a regular step size of 10°. The r_e-PES corresponds to the 3D-PES at a fixed NaH internuclear distance of $r = r_e = 3.57$ a_0 (corresponding to the experimental equilibrium geometry[30]) while the r_0-PES was calculated using a particular NaH distance of $r = r_0 = 3.61$ a_0 (corresponding to the averaged geometry). Therefore, the 3D-PES and the r_0-PES were constructed with 7410 ab initio points treated in the C_s symmetry group.

The calculations have been carried out with the explicitly correlated coupled cluster approach with single, double and perturbative triple excitation CCSD(T)-F12 in conjunction with the correlation consistent-polarized valence triple zeta cc-pVTZ Gaussian basis set[32] as implemented in the Molpro suite (version 2010)[31]. For explicitly correlated calculations, we used the the basis set mentioned above along with its corresponding default density fitting and resolution of identity functions. This methodology takes well into account the electronic correlations. As we showed in our previous papers[34,35], the potentials computed using this level of theory are similar to those obtained with the standard coupled cluster method in conjunction with a complete basis set (CBS). We have corrected the basis set superposition error BSSE with the counterpoise procedure of Boys and Bernardi[33]

$$V(r, R, \theta) = E_{NaH-He}(r, R, \theta) - E_{NaH}(r, R, \theta) - E_{He}(r, R, \theta) \quad (4)$$

The 3D-PES $V(r, R, \theta)$ obtained was then used to generate the vib-av-PES $V_{0,0}(R, \theta)$ (see equation 5).

$$V_{0,0}(R, \theta) = < \varphi_{v=0}(r) \mid V(r, R, \theta) \mid \varphi_{v'=0}(r) > \quad (5)$$

TABLE I. Comparison of computed and experimental equilibrium spectroscopic constants of NaH($X^1\Sigma^+$).

	ω_e (cm^{-1})	$\omega_e x_e$ (cm^{-1})	B_e (cm^{-1})	r_e (Å)
This work	1171.3	19.70	4.896	1.888
EXP[39]	1172.2	19.72	4.886	1.890
EXP[30]	1176.1	21.19	4.890	1.889

The 3D-PES was computed using 5 discrete values of r while the vibrational wave functions $\varphi_v(r)$ were generated with a very dense grid. Thus using directly the above equation implies to interpolate (or to truncate) the potential (the wave functions). For this purpose, we first extracted the numerical expansion routine of the 3D-PES using the fitting procedure of Werner et al. (equation 6[36]) and then derive the vib-av-PES using equation 7

$$V(r,R,\theta) = \sum_{n=1}^{N_{max}} \sum_{l=1}^{L_{max}} A_{ln}(R) d_{0,0}^{l-1}(cos\theta) \times (r-r_e)^{n-1} \quad (6)$$

$$V_{0,0}(R,\theta) = \sum_{n=1}^{N_{max}} \sum_{l=1}^{L_{max}} A_{ln}(R) d_{0,0}^{l-1}(cos\theta) \times M_{0,0}(n) \quad (7)$$

$$M_{v,v'}(n) = < \varphi_v(r) \mid (r-r_e)^{n-1} \mid \varphi_{v'}(r) >$$

where $d_{0,0}^{l-1}$ are the reduced rotation matrix of Wigner, L_{max} and N_{max} stand for the numbers of the scattering angles and the NaH internuclear distances respectively. The φ_v vibrational wave functions were computed using the Fourier Grid Hamiltonian (FGH) approach[37,38] from the NaH($X^1\Sigma^+$) interaction potential which was calculated with a RKR program[46]. To test the accuracy of the wave functions, we computed some spectroscopic constants, namely, B_e rotational constant, ω_e vibrational constant, $\omega_e x_e$ anharmonic constant and r_e equilibrium distance) of NaH($X^1\Sigma^+$) using the RKR potential. The results are compared in Tab. I to the experimental values[30,39].

We depict in Fig. 2 contour plots of the NaH-He interaction potentials as a function of θ and R (upper panel r_e-PES, middle panel r_0-PES and lower panel vib-av-PES). All these interaction potentials are visibly anisotropic and present two local minima. The global minimum D_e = 12.90 cm^{-1} occurs at R = 6.52 a_0 and $\theta = 0^\circ$ for the r_e-PES while (D_e, R, θ) = (13.06 cm^{-1}, 6.50 a_0, 0°) and (12.81 cm^{-1}, 6.55 a_0, 0°) for the r_0-PES and vib-av-PES respectively. The secondary minimum of 2.75 cm^{-1} (2.75 cm^{-1}) [2.70 cm^{-1}] is observed at R = 11.53 a_0 (R = 11.61 a_0) [R = 11.61 a_0] and $\theta = 161.60^\circ$ ($\theta = 162.30^\circ$) [$\theta = 161.4^\circ$] for the r_e-PES (r_0-PES) [vib-av-PES]. The anisotropies of the PESs displayed in Fig. 2 are thus very similar. Typically as the HCl diatomic hydride[18], the interaction potential varies slightly with the NaH bond stretching.

The computed interaction potentials (i.e. r_e-PES, r_e-PES and vib-av-PES) were then fitted using the basis

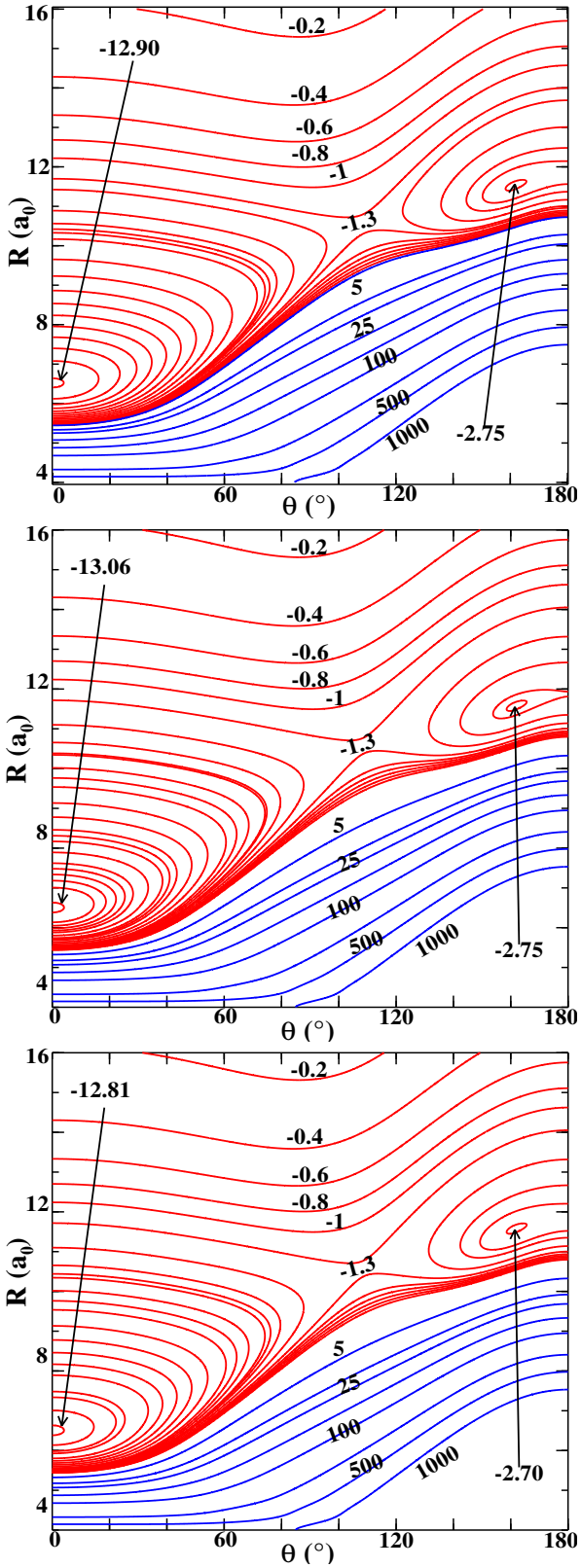

FIG. 2. Contour plots of the NaH-He interaction potentials (upper panel r_e-PES, middle panel r_0-PES and lower panel vib-av-PES) as a function of θ and R. The blue (red) contours stand for the positive (negative) energies (in unit of cm^{-1}). The zero energy corresponds to the NaH($X^1\Sigma^+$)-He(^1S) dissociation limit.

of Legendre polynomial functions including terms up to $\lambda_{max} = 18$. This yielded to the basic input V_λ(R) used in the scattering calculations.

III. SCATTERING CALCULATIONS

A. Cross sections.

Integral state-to-state rotational cross sections of NaH induced by collision with He were computed using the exact close coupling (CC) approach[40] implemented in the MOLSCAT code[41] for energies (E) ranging from 9.8 to 1500 cm^{-1}. These calculations were carried out using the modified diabatic log derivative propagator of Manolopoulos to solve the coupled equations.[42] It is worth noting that this requires to set the integration parameters of the propagator. The boundaries of the integration were set to $R_{min} = 2\ a_0$ and $R_{max} = 40\ a_0$. The STEPS parameter was set to 10 for E $\geq$ 100 cm^{-1} and to 20 for E $\leqslant$ 100 cm^{-1} as it is inversely proportional to the integration step. All these parameters were determined by carrying out some convergence tests as it is usually done. In addition, we optimized the rotational basis in order to take into account all opened channels as well as enough closed channels. Therefore, J_{max} was increased from 8 to 12 by unit at each 50 cm^{-1} for energies ranging up to 250 cm^{-1} and then $J_{max} = 13$ for 250 $\leq$ E $\leq$ 500 cm^{-1}, $J_{max} = 15$ for 500 $\leq$ E $\leq$ 1000 cm^{-1} and $J_{max} =$ 17 for 1000 $\leq$ E $\leq$ 1500 cm^{-1}. The rotational levels of NaH were computed with the usual expansion using to the experimental centrifugal distortion ($D_e = 3.32\times10^{-4}$ cm^{-1}) and rotational ($B_e = 4.9012$ cm^{-1}) constants[30] By setting the off-diagonal and diagonal tolerances to of 0.001 and 0.01 Å^2 respectively, the convergence of elastic as well as inelastic cross-sections is ensured. This led to achieve large total angular momentum (J_{tot}) values. For instance, we obtained $J_{tot} = 49$ at 100 cm^{-1}, 82 at 500 cm^{-1}, 103 for E = 1000 cm^{-1}, and 117 for E = 1500 cm^{-1}. The integral cross sections were then calculated in the energy range mentioned above by carefully increasing the grid spacing: for E $\leqslant$ 50 cm^{-1} the grid spacing was set to 0.1 cm^{-1}, for 50 $\leq$ E $\leqslant$ 100 cm^{-1} to 0.2 cm^{-1}, for 100 $\leq$ E $\leqslant$ 150 cm^{-1} to 0.5 cm^{-1}, for 150 $\leq$ E $\leqslant$ 250 cm^{-1} to 1 cm^{-1}, for 250 $\leq$ E $\leqslant$ 500 cm^{-1} to 5 cm^{-1}, for 500 $\leq$ E $\leqslant$ 1000 cm^{-1} and to 10 cm^{-1} for 1000 $\leq$ E $\leqslant$ 1500 cm^{-1}.

Fig. 3 displays the dependence on the kinetic energy of state-to-state cross sections computed using the three sets of potential presented above. Moreover, the transitions involving odd Δj values absolutely predominate in the energy range. Some few resonances are observed at low energy (mainly for the 0 $\longrightarrow$ 1 transition) despite the fine energy step used in the calculations. This may stem from the low depth of the potential wells. Such a behavior was observed for the AlH metal hydride which interacts slowly with He (the potential well is ∼26.32 cm^{-1})[43]. In fact, low potential wells hardly trap the projectile atom to form quasi-bound sates (i.e. Feshbach resonances). The shape resonances may be interpreted as quasi-bound states occurring from tunneling through the centrifugal energy barrier.

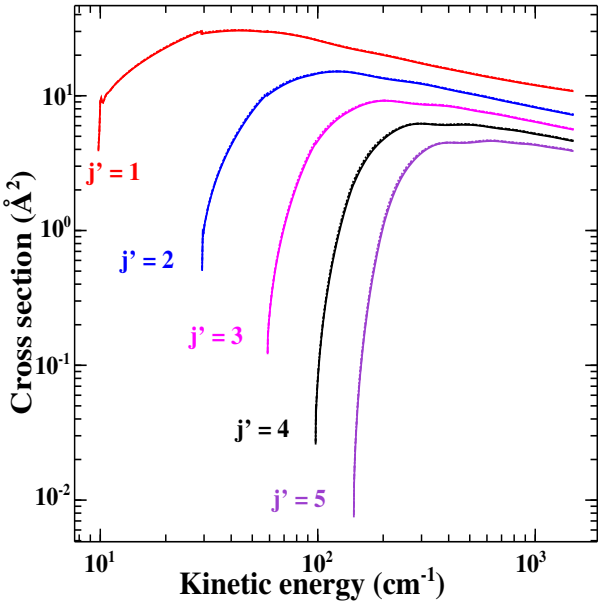

FIG. 3. Dependence on the kinetic energy of state-to-state cross sections for $0 \longrightarrow j'$ transitions. The solid lines (dashes) [dots] stand for the data computed using the vib-av-PES (r_0-PES) [r_e-PES].

We present in Fig. 4 the collisional quenching cross sections as a function of the kinetic energy. These data were generated from the vib-av-PES (lines), r_0-PES (dashes) and r_e-PES (dots). All transitions present the same shape with different magnitudes. At low kinetic energy, the $1 \longrightarrow 0$ is the largest with a value of ∼600 $Å^2$ while a propensity rule that favorites the greater j values is noted for $E_c \geq 100$ cm^{-1}.

As one can see from Fig. 3 and Fig. 4, the data computed using the three potentials overlap perfectly. This good agreement was expected since the NaH stretching has no significant effect in the interaction potentials. For a better appreciation of these agreements, see supplementary materials.

B. Collisional rates.

These cross sections were thermally averaged with the Maxwell–Boltzmann velocity distribution to compute the rate coefficients of NaH induced by collision with He. The calculations were carried out for kinetic temperatures ranging from 2 to 200 K. This enables to describe the transitions involving the 11 firsts rotational levels.

$$k_{J\longrightarrow J'}(T) = (\frac{8\beta^3}{\pi\mu})^{1/2} \int_0^\infty E_c\sigma(E_k)\mathrm{e}^{-\beta E_k}\ dE_k, \quad (8)$$

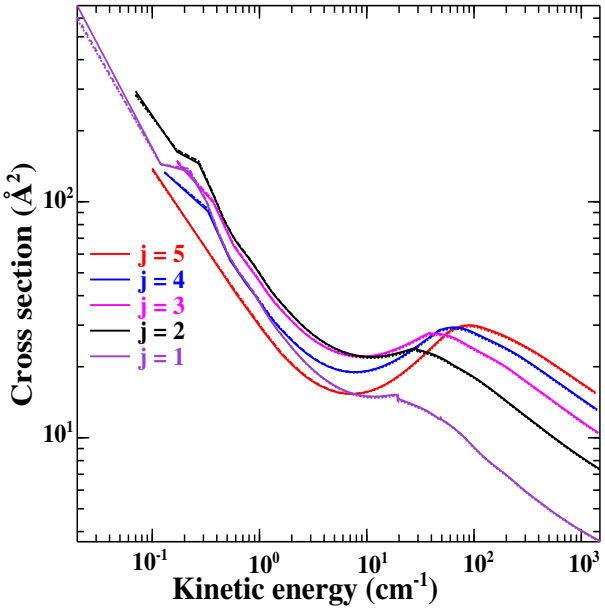

FIG. 4. Collisional quenching cross sections as a function of the kinetic energy. These data were generated from the vib-av-PES (lines), r_0-PES (dashes) and r_e-PES (dots).

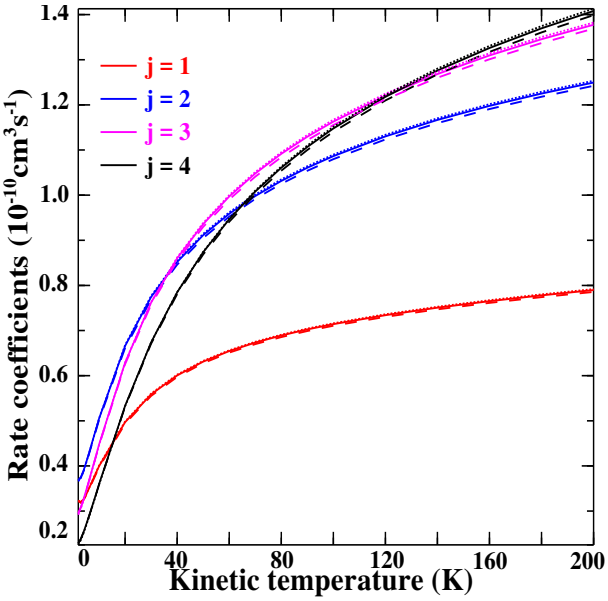

FIG. 5. Downward rate coefficients ($j \longrightarrow j-1$) as a function of the kinetic temperature. These results were computed using the vib-av-PES (lines), r_0-PES (dashes) and r_e-PES (dots).

$\beta = 1/(k_B T)$, with k_B being the constant of Boltzmann, $\mu = 3.43$ au is the reduced mass of the collisional complex, T and E_k stand for the kinetic temperature and the kinetic energy respectively. This latter was derived from the total (E) and rotational (E_J) energies. The downward collision rates were carried out for rotational transitions involving the 11 first levels.

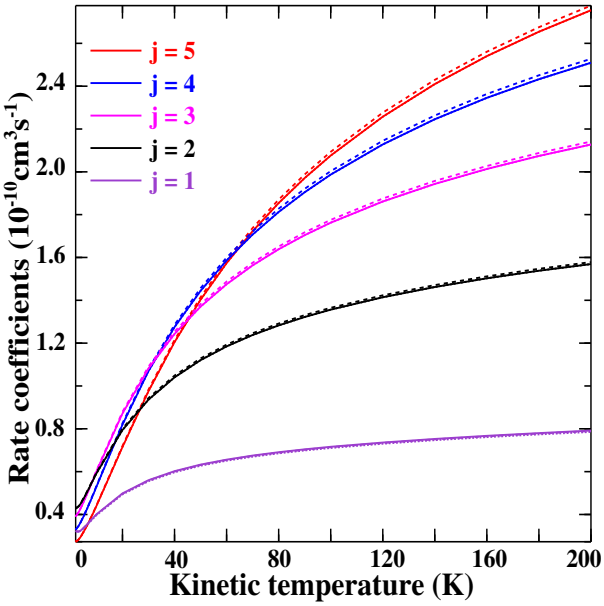

FIG. 6. Collisional quenching rate coefficients as a function of the kinetic temperature. These results were computed using the vib-av-PES (lines), r_0-PES (dashes) and r_e-PES (dots).

As cross sections predicted the dominance of transitions involving odd Δj values, we depict in Fig. 5 the rate coefficients of NaH induced by collision with He as a function of the kinetic temperature for $\Delta j = 1$ transitions. The $2 \longrightarrow 1$, $3 \longrightarrow 2$ and $4 \longrightarrow 3$ transitions outweigh the $1 \longrightarrow 0$ transition almost on the entire temperature range.

As mentioned for the quenching cross sections, the collisional quenching rates present the same shape (ascending) for all transitions drawn in Fig. 6. In addition, the magnitude decreases when j decreases for temperatures ranging from 80 K to 200 K.

Fig. 5 and Fig. 6 show that the three sets of potential lead to very close rate coefficients as observed for the cross sections. Although the perfect overlap observed for cross sections is here slightly lifted, one can conclude that the NaH vibrations do not impact significantly the rotational motions.

IV. CONCLUSIONS

In this study, we have computed three different potential energy surfaces of the NaH($X^1\Sigma^+$)-He(^1S) van der Waals system. These latter were constructed by considering that the NaH internuclear distance: is held fixed at its experimental equilibrium value, is frozen at its averaged value and varies around the classical turning points involving the three lowest vibrational levels. The calculations have been done using the explicitly correlated coupled cluster approach with simple, double and perturbative triple excitation (CCSD(T)–F12) in conjunction

with the correlation consistent–polarized valence triple zeta Gaussian basis set (cc-pVTZ) as implemented in the Molpro program (version 2010). From each of these PESs, state-to-state rotational cross sections of the alkali hydride NaH induced by collision with He have been calculated with the exact close coupling quantum mechanical approach for energies ranging up to 1500 cm^{-1}. These data were then thermally averaged over the Maxwell-Boltzmann velocity distribution to obtain downward rate coefficients for kinetic temperatures ranging from 2 to 200 K.

As noted for the HCl molecule[18], the NaH stretching impacts slightly the interaction potential. Indeed, the collisional data (cross sections and rate coefficients) computed separately from the three potentials cited above are in very good agreement. These findings may stem from the simple electronic structure of alkali hydrides. In the literature, it is recommended the use of average geometries instead of experimental equilibrium geometries. However, this conclusion stems from calculations performed mainly on charged species [SH^-[44]] and molecules in $^2\Pi$ electronic states [OH[19]]. From our findings, we suggest that equilibrium as well as average distances yield to high accurate collisional data for diatomic metal hydrides.

Concerning propensity rules, the transitions involving odd Δj values are favored for cross sections as well as for rate coefficients. These latter showed that the 2 $\longrightarrow$ 1 and 3 $\longrightarrow$ 2 transitions predominate from 60 to 200 K while the 1 $\longrightarrow$ 0 transition present a low magnitude in this temperature range. This finding may interpret the failure of the NaH tentative of detection, in diffuse clouds (TMC-1, Orion A, L134 N ρ-Ophius and Sgr B2),[24] which was focused on the 1 $\longrightarrow$ 0 rotational emission line. Therefore, we suggest to focus on the 2 $\longrightarrow$ 1 and 3 $\longrightarrow$ 2 rotational emission lines for future tentative of detection.

The data presented in this paper may be of great astrophysical interest in the detection of sodium hydride as well as in the accurate modeling of the NaH abundance in diffuse clouds. It may be also used to interpret laboratory experiments performed on cold and ultracold molecules.

[1] M. Oppenheimer and A. Dalgarno, "The fractional ionization in dense interstellar clouds," The Astrophysical Journal **192**, 29–32 (1974).

[2] G. Mitchell, "Some implications for interstellar molecules of a low electron abundance in dense clouds," The Astronomical Journal **83**, 1612 (1978).

[3] T. Snow Jr, "The depletion of interstellar elements and the interaction between gas and dust in space," The Astrophysical Journal **202**, L87–L90 (1975).

[4] W. Watson and E. Salpeter, "On the abundances of interstellar molecules," The Astrophysical Journal **175**, 659 (1972).

[5] P. J. Dagdigian, "Ground state dipole moment of nah," The Journal of Chemical Physics **71**, 2328–2329 (1979).

[6] Y.-C. Han, K.-J. Yuan, W.-H. Hu, and S.-L. Cong, "Control of photodissociation and photoionization of the nai molecule by dynamic stark effect," The Journal of chemical physics **130**, 044308 (2009).

[7] P. Backhaus and B. Schmidt, "Femtosecond quantum dynamics of photoassociation reactions: the exciplex formation of mercury," Chemical physics **217**, 131–143 (1997).

[8] J. M. Sage, S. Sainis, T. Bergeman, and D. DeMille, "Optical production of ultracold polar molecules," Physical review letters **94**, 203001 (2005).

[9] S. Qian-Zhen, Y. Jie, N. Ying-Yu, and C. Shu-Lin, "Rovibrational formation of ultracold nah molecules induced by an ultrashort laser pulse," Chinese Physics Letters **27**, 093401 (2010).

[10] P. Dagdigian, "Detection of lih and nah molecular beams by laser fluorescence and measurement of radiative lifetimes of the a $1\sigma+$ state," The Journal of Chemical Physics **64**, 2609–2615 (1976).

[11] H.-Y. Huang, T.-L. Lu, T.-J. Whang, Y.-Y. Chang, and C.-C. Tsai, "Dissociation energy of the ground state of nah," The Journal of chemical physics **133**, 044301 (2010).

[12] C.-C. Chu, W.-F. He, R.-S. Lin, Y.-J. Li, T.-J. Whang, and C.-C. Tsai, "Spectroscopic determination of the ground-state dissociation energy and isotopic shift of nad," The Journal of Chemical Physics **147**, 024301 (2017).

[13] A. Belyaev, J. Grosser, J. Hahne, and T. Menzel, "Ab initio cross sections for low-energy inelastic h+ na collisions," Physical Review A **60**, 2151 (1999).

[14] A. Dickinson, R. Poteau, and F. Gadéa, "An ab initio study of mutual neutralization in na++ h-collisions," Journal of Physics B: Atomic, Molecular and Optical Physics **32**, 5451 (1999).

[15] M. Motzkus, G. Pichler, K. Kompa, and P. Hering, "Local laser superheating due to quenching determined by degenerate four-wave-mixing and absorption thermometry," Chemical physics letters **257**, 181–189 (1996).

[16] M. Motzkus, G. Pichler, K. Kompa, and P. Hering, "Vibrationally induced formation of nah in the na (3p)+ h 2 collision system: Rate equation model and comparison with experimental results," The Journal of chemical physics **108**, 9291–9300 (1998).

[17] M. D. Hack and D. G. Truhlar, "Analytic potential energy surfaces and their couplings for the electronically nonadiabatic chemical processes na (3p)+ h 2→ na (3s)+ h 2 and na (3p)+ h 2→ nah+ h," The Journal of chemical physics **110**, 4315–4337 (1999).

[18] M. Lanza and F. Lique, "Collisional excitation of interstellar hcl by he," Monthly Notices of the Royal Astronomical Society **424**, 1261–1267 (2012).

[19] Y. Kalugina, F. Lique, and S. Marinakis, "New ab initio potential energy surfaces for the ro-vibrational excitation of oh (x 2 π) by he," Physical Chemistry Chemical Physics **16**, 13500–13507 (2014).

[20] N. Bouhafs, F. Lique, A. Faure, A. Bacmann, J. Li, and H. Guo, "Rotational excitation of the interstellar nh2 radical by h2," The Journal of Chemical Physics **146**, 064309 (2017).

[21] D. C. Morton, "Interstellar absorption lines in the spectrum of zeta ophiuchi," The Astrophysical Journal **197**, 85–115 (1975).

[22] T. Snow Jr and W. H. Smith, "A search for interstellar nah in diffuse clouds," The Astrophysical Journal **217**, 68–70 (1977).

[23] J. Czarny, P. Felenbok, and E. Roueff, "A search for interstellar nah and mgh in diffuse clouds," Astronomy and astrophysics **188**, 155–158 (1987).

[24] R. Plambeck and N. Erickson, "A search for nah in dense molecular clouds-evidence against formation on grains," The Astrophysical Journal **262**, 606–610 (1982).

[25] F. Combes and T. Wiklind, "Search for lih in the ism towards b0218+ 357," arXiv preprint astro-ph/9804303 (1998).

[26] D. Friedel, A. Kemball, and B. D. Fields, "The search for extragalactic lithium hydride," The Astrophysical Journal **738**, 37 (2011).

[27] B. K. Taylor, "A three-dimensional he-nah potential energy surface for rovibrational energy transfer studies," The Journal of chemical physics **121**, 7725–7734 (2004).

[28] M. Cafiero, L. Adamowicz, M. Duran, and J. M. Luis, "Nonadiabatic and born–oppenheimer calculations of the polarizabilites of lih and lid," Journal of Molecular Structure: THEOCHEM **633**, 113–122 (2003).

[29]J. M. Martin, "Ab initio total atomization energies of small molecules—towards the basis set limit," Chemical physics letters **259**, 669–678 (1996).
[30]M. Giroud and O. Nedelec, "Spectroscopy of the nah, nad, kh, and kd x $1\sigma+$ ground state by laser excited fluorescence in a high frequency discharge," The Journal of Chemical Physics **73**, 4151–4155 (1980).
[31]H.-J. Werner, P. Knowles, G. Knizia, F. Manby, M. Schütz, P. Celani, T. Korona, R. Lindh, A. Mitrushenkov, G. Rauhut, *et al.*, "Molpro, version 2010.1, a package of ab initio programs," See http://www. molpro. net (2010).
[32]T. H. Dunning Jr, "Gaussian basis sets for use in correlated molecular calculations. i. the atoms boron through neon and hydrogen," The Journal of chemical physics **90**, 1007–1023 (1989).
[33]S. F. Boys and F. d. Bernardi, "The calculation of small molecular interactions by the differences of separate total enegies. some procedures with reduced errors," Molecular Physics **19**, 553–566 (1970).
[34]C. T. Bop, K. Hammami, A. Niane, N. Faye, and N. Jaïdane, "Rotational excitation of 36arh+ by he at low remperature," Monthly Noticies of the Royal Astronomical Society **465**, 1137–1143 (2017).
[35]C. T. Bop, K. Hammami, and N. Faye, "Collisional rates based on the first potential energy surface of the neh+- he system." Monthly Notices of the Royal Astronomical Society (2017).
[36]H.-J. Werner, B. Follmeg, and M. H. Alexander, "Adiabatic and diabatic potential energy surfaces for collisions of cn (x $2\sigma+$, a 2π) with he," The Journal of chemical physics **89**, 3139–3151 (1988).
[37]G. G. Balint-Kurti, R. N. Dixon, and C. C. Marston, "Grid methods for solving the schrödinger equation and time dependent quantum dynamics of molecular photofragmentation and reactive scattering processes," International Reviews in Physical Chemistry **11**, 317–344 (1992).
[38]C. C. Marston and G. G. Balint-Kurti, "The fourier grid hamiltonian method for bound state eigenvalues and eigenfunctions," The Journal of Chemical Physics **91**, 3571–3576 (1989).
[39]R. Pankhurst, "The emission spectrum of sodium hydride," Proceedings of the Physical Society. Section A **62**, 191 (1949).
[40]A. Arthurs and A. Dalgarno, "The theory of scattering by a rigid rotator," in *Proceedings of the Royal Society of London A: Mathematical, Physical and Engineering Sciences*, Vol. 256 (The Royal Society, 1960) pp. 540–551.
[41]J. Hutson and S. Green, "Molscat computer code, version 14," Collaborative computational project (1994).
[42]D. Manolopoulos, "An improved log derivative method for inelastic scattering," The Journal of chemical physics **85**, 6425–6429 (1986).
[43]M. Pamboundom, J. Fifen, C. Nkem, and M. Nsangou, "Rotational excitation of alh by helium and neon at low temperature: State-to-state inelastic cross section," Chemical Physics Letters **600**, 21–28 (2014).
[44]C. Bop, T. Trabelsi, K. Hammami, M. Mogren Al Mogren, F. Lique, and M. Hochlaf, "Cold collisions of sh- with he: Potential energy surface and rate coefficients," The Journal of Chemical Physics **147**, 124301 (2017).
[45]A. Niane, K. Hammami, F. NAB, and N. Jaidan, "Ab initio potential energy surface and rotational inelastic collisions of hydroxide of lithium (lih) with argon (ar): State-to-state inelastic rotational cross section," Computational and Theoretical Chemistry **933**, 20–25 (2012).
[46]R. LeRoy, "University of Waterloo chemical physics research report cp657r, 2004," http://scienide2.uwaterloo.ca/~rleroy/rkr/, accessed: 2017-10-14.
[47]F. Gianturco, S. Kumar, S. K. Pathak, M. Raimondi, and M. Sironi, "Interaction forces and energy transfer dynamics of lih ($x^1\sigma^+$) and helium atoms ii. rotationally inelastic collisions and excitation efficiency," Chemical Physics **215**, 239–252 (1997).
[48]L. Wharton, L. P. Gold, and W. Klemperer, "Preliminary values of some molecular constantsof lithium hydride," The Journal of Chemical Physics **37**, 2149–2150 (1962).